JOURNAL OF VIROLOGY, Apr. 1999, p. 3190–3196 Vol. 73, No. 4
0022-538X/99/$04.00+0

Distinct Attenuation Phenotypes Caused by Mutations in the Translational Starting Window of Theiler's Murine Encephalomyelitis Virus

EVGENY V. PILIPENKO,[1,2] EKATERINA G. VIKTOROVA,[1] ELENA V. KHITRINA,[1] SVETLANA V. MASLOVA,[1] NADINE JAROUSSE,[3] MICHEL BRAHIC,[3] AND VADIM I. AGOL[1,2]*

Institute of Poliomyelitis and Viral Encephalitides, Russian Academy of Medical Sciences, Moscow Region 142782,[1] and Moscow State University, Moscow 119899,[2] Russia, and Unité des Virus Lents, ERS 572 CNRS, Institut Pasteur, 75724 Paris Cedex 15, France[3]

Received 10 September 1998/Accepted 8 December 1998

Upon initiation of translation of picornavirus RNA, the ribosome is believed to bind the internal ribosome entry site of the template and then to form a productive complex with a downstream RNA segment, the starting window. The presence or absence of an AUG triplet within the starting window of the RNA of Theiler's murine encephalomyelitis virus (a picornavirus) is known to modulate its neurovirulence. In this study, mutants of this virus in which the starting windows, lying upstream of the viral polyprotein reading frame, had AUGs with different nonoptimal contexts were engineered. Upon intracerebral inoculation of mice, the mutants proved to be partially attenuated, as judged by a significant increase in the dose causing paralysis in 50% of the animals (PD_{50}). Mutants with similar PD_{50}s might differ from one another by eliciting either a severe, fatal tetraplegy or only mild, recoverable neurologic lesions. Some of the mutants triggered a chronic inflammatory reaction in the white matter of the spinal cord in the absence of detectable viral RNA or antigen. Thus, point mutations changing the context of an AUG within the starting window outside the polyprotein reading frame may differently affect the morbidity and mortality caused by a viral infection and may result in distinct attenuation phenotypes.

The neurovirulence of a virus depends on a variety of genetic determinants. In picornaviruses, naked icosahedral viruses with a single-stranded 7.5- to 8-kb RNA genome of positive polarity (25), a set of such determinants maps to the 5′ untranslated region (5UTR) of the RNA and is related to the translational control (26, 27; reviewed in references 2 and 3). Numerous studies demonstrated that modifications of these determinants may result in different levels of attenuation of viral pathogenicity. The major aim of the present report is to document that certain point mutations within a translational *cis*-acting element in the 5UTR of a picornavirus, Theiler's murine encephalomyelitis virus (TMEV), not only lower the viral virulence quantitatively but may result in distinct clinical patterns.

Under natural conditions, TMEV normally causes asymptomatic enteric infection. However, upon intracerebral inoculation of mice, it exhibits strong neuropathogenicity. Depending on the strain, the infection results in either an acute paralytic and lethal encephalomyelitis (e.g., in mice infected with the GDVII strain) or a persistent demyelinating disease (BeAn or DA strains), with this difference being attributed to point mutations in viral capsid proteins (references 1, 10, 16, and 18 and references therein). TMEV is widely used as a model pathogen to study a variety of aspects of viral neurovirulence as well as pathogenesis of human diseases, e.g., multiple sclerosis (7, 17, 20, 28).

The reproduction of TMEV, like that of other picornaviruses, involves 5′ cap-independent internal initiation of translation promoted by a *cis*-acting element, the internal ribosome entry site (IRES) (reviewed in references 2, 9, and 29). This highly structured (21) element, which is several hundred nucleotides long, is located within the viral RNA 5UTR. The ribosome (or its 40S subunit) is believed to bind the IRES and to form a productive contact with a downstream segment, the starting window, of the RNA template (23). In TMEV, the starting window comprises about 12 nucleotides (nt) and lies about 17 nt downstream of the IRES (23). After contacting the starting window, the ribosome begins translation of the viral polyprotein from an initiator AUG that lies within the window and has a favorable context (purine residues at positions −3 and +4 relative to the first nucleotide of the AUG).

To define the properties of the starting window, AUG-lacking insertions between the TMEV (GDVII) IRES and the initiator codon have been engineered (23). These insertions, while displacing the latter from the starting window, did not markedly affect viral reproduction in BHK-21 cells or translation of its RNA in some cell-free systems. The ribosomes appeared to scan the template from the starting window until a downstream good-context AUG was encountered (23). On the other hand, the same insertions resulted in a dramatic loss of neurovirulence (24). The viruses isolated from the brains of rare paralyzed animals exhibited virulent phenotypes and contained either deletions or AUG-generating point mutations, both returning an AUG to the starting window (24). Neurovirulence was nearly fully or partially restored when an AUG in a favorable or unfavorable context, respectively, was introduced into the starting window (24). While the good-context AUG slightly extended the open reading frame (ORF) of the viral polyprotein by adding nine in-frame codons, the poor-context AUGs of these mutants could not serve for polyprotein initiation because an in-frame termination codon was placed between this triplet and the polyprotein ORF. In the course of that study, it was noticed that the clinical patterns elicited by

* Corresponding author. Mailing address: Institute of Poliomyelitis, Moscow Region 142782, Russia. Phone: 7 (95) 439 90 26. Fax: 7 (95) 439 93 21. E-mail: viago@ipive.genebee.msu.su.

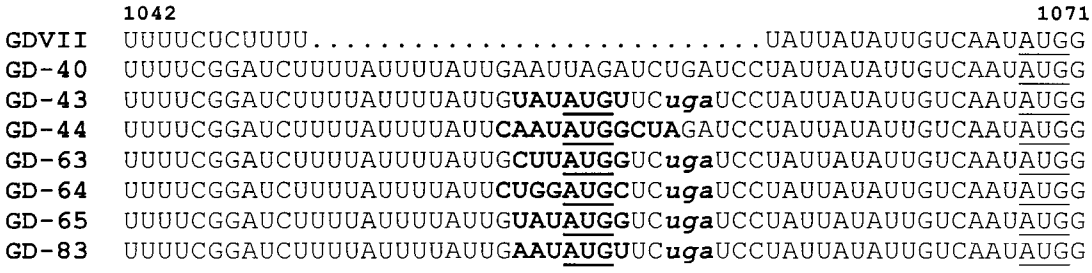

FIG. 1. Genome structures of GDVII and its derivatives. Dots in the GDVII sequence are for alignment. AUGs are underlined. For the mutants with the 27-nt inserts, the AUG and its variable contexts within the starting window are in boldface and the stop codon that follows is in italics.

mutants with different poor AUG contexts may differ from one another. This notion, if correct, should have important implications. It may suggest that point mutations within a control element of the 5UTR may modulate clinical signs of a neurologic disease. Furthermore, laboratory characterization of pathogenic strains may in this case require exact knowledge of the primary structure of a certain region of the 5UTR. Taking into the account these considerations, we constructed a novel set of GDVII TMEV mutants having different unfavorable contexts of the AUG within the starting window followed by a stop codon. These mutations could be expected to affect the formation of the ribosome-template productive complex, whereas the viral polyprotein should be initiated at its cognate site. The mutants proved to be similar to each other and to the wild-type (wt) virus in their in vitro phenotypes and were all attenuated to a certain extent. Remarkably, these mutants differed markedly from each other in the clinical signs of the disease they induced, even though the paralytogenic doses (doses causing paralysis in 50% of the animals [PD_{50}s]) for some of these mutants were almost the same. Thus, point mutations within the starting window outside the polyprotein ORF may differently affect the morbidity and mortality caused by a viral infection and may result in distinct attenuation phenotypes.

MATERIALS AND METHODS

Mice. BALB/c, CBA, and C57/BL mice were obtained from the Animal House of the Russian Academy of Medical Sciences (Stolbovaya, Moscow Region, Russia); SJL/J mice were from the Institut Pasteur (Paris, France).

Construction of mutant viruses. Plasmid GD-43 and the corresponding mutant virus (mutant 43) have been described previously (23). New mutants were engineered by oligonucleotide-directed mutagenesis with the pUGD/I.27-40 intermediate construct, and the viruses were recovered from transcript RNA-transfected BHK-21 cells as described previously (23). In vitro and in vivo viral phenotypic properties were determined as described previously (24).

Construction and translation of luciferase-expressing plasmids. The pGLV intermediate construct was generated by ligation of a *Hin*dIII/*Bam*HI fragment of GD-2 (23), containing a pUC vector sequence and nt 1 to 1047 of the GDVII cDNA under the control of a T7 promoter, to a *Bam*HI/*Hin*dIII fragment of pBLC (a plasmid kindly donated by T. D. K. Brown), containing the luciferase cDNA sequence (nt 22 to 1841) and a polylinker. PCR-amplified TMEV DNA fragments (nt 779 to 1122) were derived from the wt and mutant plasmids. *Kpn*I-digested fragments (nt 937 to 1122) were ligated to pGLV, which was linearized with *Bam*HI (at position 1047), filled in with the Klenow enzyme, and digested with *Kpn*I (at position 937). The resulting pLG constructs contained, under control of the T7 promoter, the entire wt or mutant GDVII 5UTRs and an ORF starting at the TMEV initiator AUG_{1068} followed by 28 codons, mostly of viral origin, fused in frame to the luciferase gene.

pLG plasmids were linearized with *Hin*dIII, and transcription was carried out as described previously (22). The transcripts were precipitated with 2 M LiCl and then with ethanol, RNA was dissolved in water, and its concentration was determined spectrophotometrically. RNA aliquots were stored at −70°C and were thawed only once. For translation in reticulocyte lysates, the pLG transcripts (20 μg/ml) were incubated at 30°C for 1 h under the conditions described previously (23). The template activity was quantified by the measurement of [^{35}S]methionine incorporation into the luciferase band separated by sodium dodecyl sulfate-polyacrylamide gel electrophoresis. For the in vivo translation, 1-day-old quadruplicate cultures of BHK-21 cells grown in 50-mm-diameter plastic dishes were each transfected with 2 μg (saturating amount) of pLG transcripts by the DEAE-dextran method (23). After a 3-h incubation at 37°C, when the accumulation of luciferase reached peak values, cells were removed and the luciferase activity was determined by using the Promega Luciferase Assay System according to the manufacturer's protocol. The signals were normalized to 10^6 cells by determining the protein concentration in the lysates by the Lowry method. The signal variation in quadruplicate cultures did not exceed 15% of the average value for a given template. The saturating amount of RNA in this assay corresponded to 1 μg/dish.

Characterization of viral genomes in mouse brains. The presence of the viral genome in the central nervous system (CNS) was evaluated by dot blot hybridization. Anesthetized mice were perfused through the left ventricle with 20 ml of phosphate-buffered saline (PBS), and their brains and spinal cords were immediately removed. Total RNA was extracted (6) and quantified spectrophotometrically. Four serial fivefold dilutions of total RNA from the brain and spinal cord of each mouse were dot blotted on Hybond C-extra filters (Amersham), starting with 10 μg per dot, and hybridized with a ^{32}P-labeled DNA probe corresponding to the viral sequence from nt 5437 to 6914 generated by random priming. Hybridization of the same material with a β-actin probe was carried out as a control.

The structure of the viral genomes in brains was characterized as described previously (24). The characterization included reverse transcription-PCR (RT-PCR) amplification of the appropriate region of the viral RNA (between positions 779 and 1214 of the wt GDVII sequence), determination of the lengths and sequences of the relevant fragments, and, in the case of heterogeneity, cloning into a plasmid followed by sequencing.

Histopathology and immunofluorescence. Anesthetized mice were perfused with 20 ml of PBS followed by 20 ml of 4% paraformaldehyde in PBS. Dissection of the CNS, postfixation, and paraffin embedding were performed as described previously (4). Sections of brains and longitudinal sections of spinal cords were examined for histopathology by hematoxylin staining. Viral antigens were detected with a rabbit anticapsid serum, a secondary biotinylated goat anti-rabbit immunoglobulin, and the LSAB peroxidase kit (DAKO, Carpinteria, Calif.).

RESULTS

Genome structures of the mutants and their in vitro properties. The structure of the relevant region of the TMEV (GDVII strain) genome is presented in Fig. 1. All of the mutants used here contained a nonviral 27-nt insertion between the IRES and the initiator AUG_{1068}, which by itself did not appreciably change the in vitro phenotype of the virus (23) but modulated its neurovirulence, depending on whether an AUG was present within the insert (24). The absence of AUG (mutant 40 [Fig. 1]) was accompanied by a nearly complete loss of virulence ($\log_{10}$ PD_{50} = 7.7), whereas the presence of AUG in an optimal context (aauAUGg; in mutant 44) resulted in no marked change compared to that of the wt GDVII ($\log_{10}$ PD_{50}s of 3.7 and 2.5, respectively); a poor AUG context (uau AUGu; mutant 43) resulted in an intermediate level of attenuation ($\log_{10}$ PD_{50} = 5.2) (24). The suboptimal-context AUG within the starting window of the mutants could not serve to initiate the viral polyprotein, even inefficiently, because a terminator UGA was present 3 nt downstream.

The inserts in the newly engineered mutants also had AUG codons in nonoptimal (but different) contexts followed by stop

TABLE 1. GDVII viruses and their properties

Virus	Relative template activity		Plaque size (mm)	PD_{50} (log_{10} TCD_{50})
	RRL[a]	BHK-21		
GDVII	1.00	1.00	1.7	2.9
Mutants				
43	0.53	0.68	1.5	5.1
63	0.37	0.48	1.5	4.9
64	0.42	0.53	1.4	5.7
65	0.61	0.74	1.5	5.0
83	0.58	0.52	1.3	>8.0

[a] RRL, rabbit reticulocyte lysate.

codons, with the changes affecting 3 or 4 nt upstream and 1 nt downstream of this triplet (Fig. 1). The growth of the mutants in BHK-21 cells was not significantly altered by these variations, as judged by the plaque size (Table 1). The effects of mutations on the RNA template activities were assayed both in vitro (reticulocyte lysates) and in vivo (BHK-21 cells), using constructs in which the mutated 5UTRs were fused to the luciferase gene. [^{35}S]methionine incorporation into the luciferase polypeptide chain and luciferase activity were determined in the in vitro and in vivo experiments, respectively (see Materials and Methods). In both assays, the translatability of the mutant RNAs, although slightly diminished, comprised about 40 to 60% and 50 to 75%, respectively, of the wt RNA value and did not appreciably depend on the AUG context (Table 1).

Neurovirulence and clinical patterns. When tested for virulence by intracerebral inoculation of BALB/c mice, all of the mutants except mutant 83 could be assigned to a single set, having PD_{50} values 10^2 to 10^3 higher than that of the wt GDVII (Table 1). Despite this similarity, these mutants could be considered to belong to two groups that were dramatically different in the pattern of clinical signs they induced. Once paralyzed, a mouse inoculated with mutant 63 (cuuAUGg) was prone to develop, like a wt-infected mouse, a severe paralytic disease (e.g., tetraplegy) and had a very high chance of dying within 1 to 2 weeks postinoculation (p.i.) (generally 2 to 3 days after the appearance of the first clinical signs) (Fig. 2). Rare survivors did not recover from the neurologic disease during the observation period (7 to 10 weeks) (Fig. 3). A similar, although slightly milder, clinical pattern was characteristic of mice inoculated with mutant 65 (uauAUGg) (Fig. 3). On the other hand, the disease caused by the representatives of the second group of mutants, mutants 43 (uauAUGu) and 64 (ug gAUGc), was less severe: the overwhelming majority (≥85%) of the diseased mice did survive, and a significant proportion of them appeared to completely recover by the end of the seventh week (Fig. 2 and 3). The rare deaths occurred only after many days of disease and was likely caused by revertants (see below).

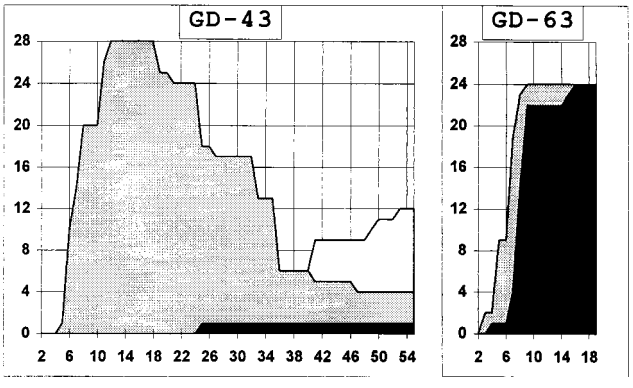

FIG. 2. Time course of clinical signs after intracerebral inoculation of mice with mutants 43 and 63 at 10^8 and $10^{8.5}$ TCD_{50}, respectively. Twenty-eight and 24 animals were infected simultaneously with mutants 43 and 63, respectively, and monitored individually. The numbers of mice that were paralyzed, died, and developed the second wave of paralytic symptoms are shown as gray, black, and white areas, respectively. Numbers on the *x* axis are days p.i.

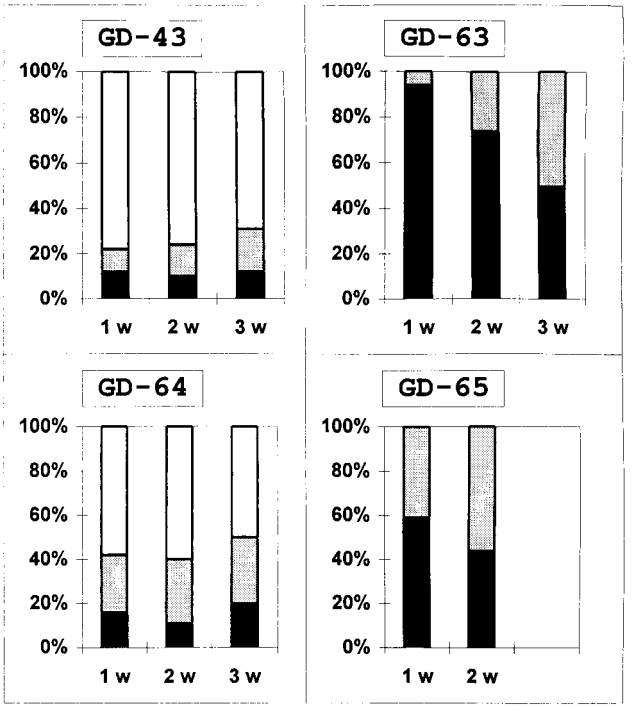

FIG. 3. Dependence of the outcome of infection by 7 to 10 weeks p.i. on the time of the appearance of the first clinical signs. The proportions of dead (black bars), irrecoverably paralyzed (gray), and fully recovered (white) mice are shown. Data were collected from several experiments. The numbers of animals that got sick during the first (1 w), second (2 w), and third (3 w) weeks, respectively, were as follows: 72, 70, and 26 (mutant 43); 66, 34, and 8 (mutant 63); 38, 35 and 10 (mutant 64); and 29, 9, 0 (mutant 65).

In the case of GDVII and mutant 63, half of the mice inoculated with doses close to the PD_{50} and two log units higher got sick at between 11 and 12 and between 6 and 7 days p.i., respectively, whereas these values corresponded to 17 to 18 and 8 to 9 days for mutant 43. The earlier that neurologic signs of the disease caused by mutants 63 and 65 became apparent, the greater was the probability of a lethal outcome (Fig. 3). However, this was not the case with mutants 43 and 64, where the mortality was low even when the clinical signs became apparent relatively early, and no correlation between the time of the onset of the disease and its prognosis could be noted (Fig. 3). In some experiments with mutant 43, a few mice, after a period of apparent recovery, developed a second wave of paralytic symptoms at 40 to 50 days p.i. (Fig. 2).

Mutant 83 (aauAUGu) turned out to be strongly attenuated, inducing no clinical signs at the highest inoculation dose (10^8 tissue culture infective doses [TCD_{50}]) tested (Table 1).

Limited neurovirulence tests were also carried out with CBA and C57/BL mice. Again, mutants 43 and 64 invariably caused a milder course of the disease than that with mutant 63. How-

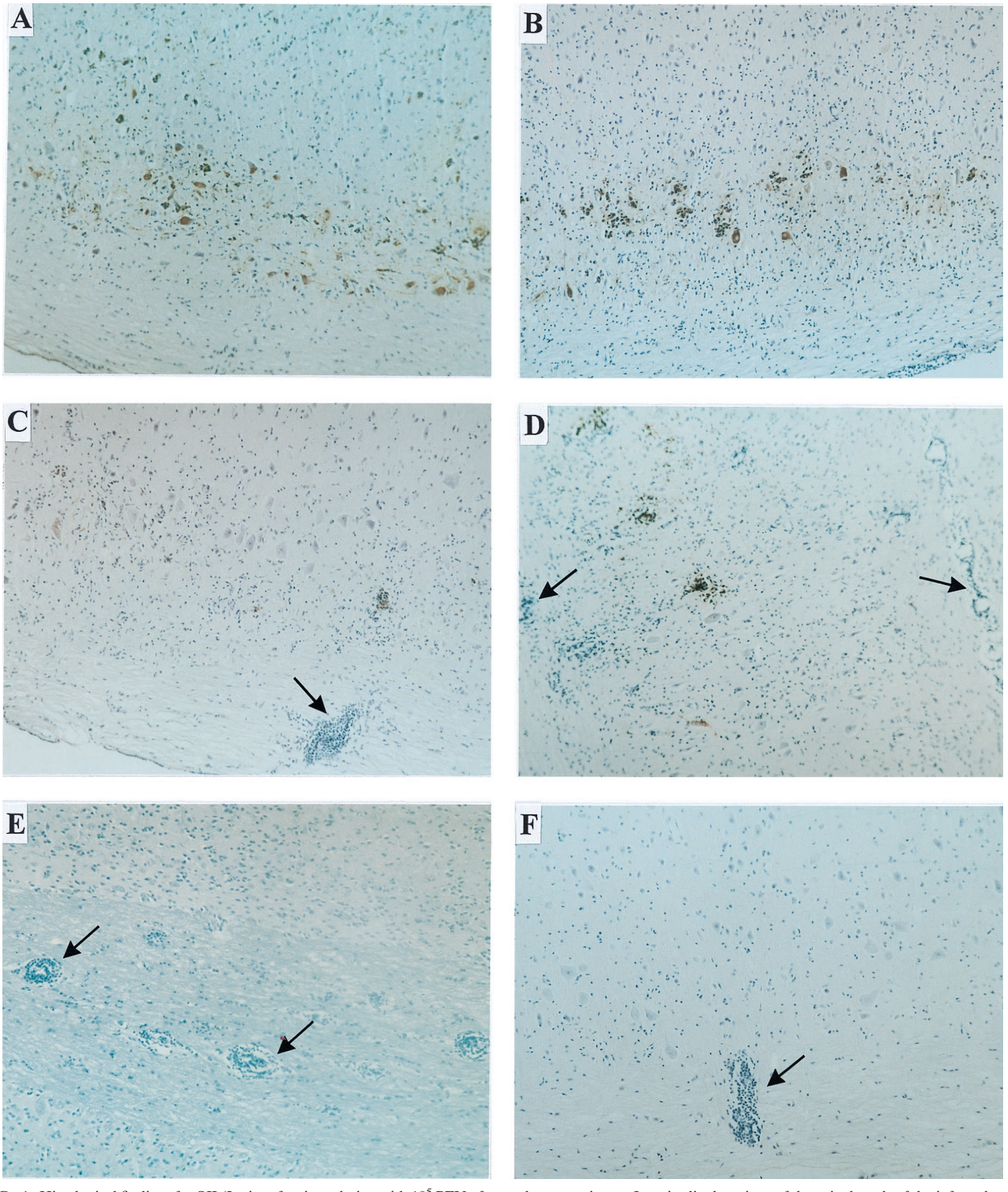

FIG. 4. Histological findings for SJL/J mice after inoculation with 10^5 PFU of wt and mutant viruses. Longitudinal sections of the spinal cords of the infected animals were prepared on day 5 for GDVII (A) on day 6 for mutants 63 (B), 64 (C), and 43 (D), and on day 22 for mutant 43 (E and F). Viral antigens were detected by the immunoperoxidase assay with a polyclonal anti-TMEV rabbit serum (brown clusters). Virus-infected cells were localized in the gray matter and were more abundant in the GDVII- and mutant 63-infected animals than in the mutant 43 and 64 infections. In the case of mutants 43 and 64 (but not in the case of GDVII and mutant 63), there were marked signs of inflammation in the white matter (arrows) even at day 22 p.i., when no viral antigen was detectable (E and F). Magnification, ×312.

ever, in CBA mice, as distinct from BALB/c and C57/BL mice, the PD_{50}s of the former viruses were significantly higher than that of mutant 63 (not shown).

Viral antigen and RNA accumulation. The variation in the clinical patterns induced by the mutants correlated well with the viral antigen accumulation in the CNS. At days 5 to 6 p.i., numerous antigen-containing cells, apparently neurons, could be seen in the gray matter of the brains and spinal cords of GDVII- and mutant 63-infected SJL/J mice, whereas such cells were much less abundant in the diseased mice inoculated with

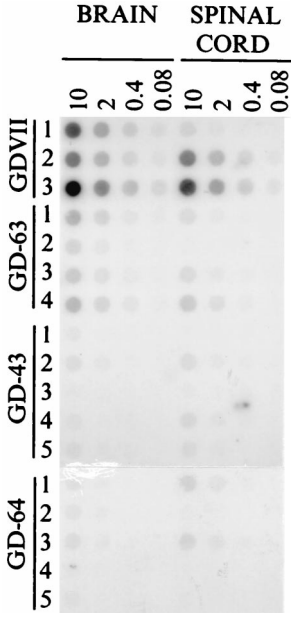

FIG. 5. Viral RNA in the CNSs of infected mice as assayed by dot blot hybridization. GDVII- and mutant-infected mice were sacrificed on days 5 and 6 p.i., respectively. Total cytoplasmic RNA was extracted from the brains and spinal cords of infected mice, loaded on the membrane (in the amounts [in micrograms] indicated at the top) and hybridized with ^{32}CTP-labeled PCR-amplified, virus-specific DNA. The numbers on the left correspond to individual mice.

mutants 43 and 64 (Fig. 4). The viral antigen disappeared nearly completely by 8 to 11 days. Very few, if any, antigen-containing cells could be detected in the white matter of the surviving mice at any time of infection with any of the viruses investigated.

The virus-specific RNA in the CNSs of the mutant-infected SJL/J mice was assayed by dot blot hybridization (Fig. 5). At day 6, signals observed in the mutant 63-inoculated animals, especially in the brain, were somewhat higher than in the case of mutants 43 and 64. At day 14, the viral RNA in the CNSs of survivors could no longer be detected or was present in trace amounts (not shown). After 6 weeks p.i., viral RNA could not be detected (with very rare exceptions) in mice of any strain even by the RT-PCR assay (not shown).

Pathological findings. Early upon infection with GDVII or mutant 63, there was a weak inflammatory reaction in the gray matter and meningea and nearly no such reaction in the white matter (Fig. 4). However, with mutants 64 and, especially, 43 there were marked signs of inflammation in the white matter (Fig. 4), even though it contained very little, if any, detectable viral antigen. In the gray matter, the distributions of the antigen-containing cells and inflammatory loci mostly did not coincide with each other either. Marked inflammation in the white matter of mutant 43-infected mice could be seen at day 22 (when the antigen was no longer detectable even in the gray matter) (Fig. 4) and at day 45, although at this time it was less pronounced (not shown). A qualitatively similar inflammatory reaction was also characteristic of mutant 64-infected mice (not shown). Comparable, although somewhat milder, patterns of distribution of antigen-containing cells and inflammation were found also in the CNSs of the mutant-infected BALB/c mice (not shown).

Genome structures of the viruses in the CNSs of diseased mice. Sequencing of the relevant region of the viral genome revealed no additional mutations (other than those engineered) in the RNAs of the more virulent mutants 63 and 65 in the severely paralyzed or dead animals (Table 2). In the case of mutants 43 and 64, mice with a typical (mild) clinical pattern also harbored the parental viral genome, whereas pseudoreversions (deletions) returning the cognate initiator AUG to the starting window were found in the CNSs of the mice exhibiting

TABLE 2. GDVII viruses isolated from mouse CNS and their genome structures

Mutant virus	Isolate	Day	Clinical stage[a]	Sequence[b]
43	19	8	PP of hind limbs	^{1046}CGGAUCUUUUAUUUUAUU**GUAUAUGU**UCUGAUCCUAUUAUAUUGUCAAUAUG^{1070}
	107	9	PP of limbs	Parental
	43K	36	PP of hind limbs	Parental
	43E	33	FP of hind limbs	^{1046}CGGAUCUUUU**********UUAUAUUGUCAAUAUG^{1070}
	88[c]	20	Death	^{1046}CGGAUCUU**********UUAUAUUGUCAAUAUG^{1070}
63	108	9	FP of limbs	^{1046}CGGAUCUUUUAUUUUAUU**GCUUAUGG**UCUGAUCCUAUUAUAUUGUCAAUAUG^{1070}
	109	9	FP of limbs	Parental
	296	7	Death	Parental
	301	8	Death	Parental
64	64K	14	PP of hind limbs	^{1046}CGGAUCUUUUAUUUUAUU**CUGGAUGC**UCUGAUCCUAUUAUAUUGUCAAUAUG^{1070}
	113	14	Death	^{1046}CGGAUCUUUUAUU**********UAUUGUCAAUAUG^{1070}
	116	16	Death	^{1046}CGGAUCUU**********UUAUAUUGUCAAUAUG^{1070}
	185	20	Death	^{1046}CGGAUCUUUUAUUUU**********UAUUGUCAAUAUG^{1070}
	234[c]	13	FP of limbs	^{1046}CGGAU**********CUAUUAUAUUGUCAAUAUG^{1070}
65	299	7	PP of hind limbs	^{1046}CGGAUCUUUUAUUUUAUU**GUAUAUGG**UCUGAUCCUAUUAUAUUGUCAAUAUG^{1070}
	300	9	Death	Parental
	324	29	Death	Parental

[a] PP, partial paralysis; FP, full paralysis.

[b] For each virus, the first sequence is the parental sequence. The AUG within the starting window with its context is in boldface. The initiator AUG is underlined. Deleted nucleotides are indicated by asterisks. RNAs were extracted either (i) from BHK-21 cells, after accumulation of viruses isolated from mice brains, for 43E, 299, and 324 or (ii) directly from mice brains for the other isolates.

[c] The isolate contained a mixture of the parental genome and the revertant one.

more grave clinical signs or dead animals, as revealed by sequencing (Table 2) and RT-PCR length polymorphism (not shown).

DISCUSSION

The results described above demonstrate that the target cells in the CNS, presumably neurons, may discriminate between different nonoptimal contexts of an upstream AUG within the starting window, even though no marked discrimination could be demonstrated in either BHK-21 cells or some cell-free translation systems. Most likely, this discrimination occurs at the level of translation initiation, but the mechanism of the AUG context recognition remains unknown. If the poor-context AUG within the insert was still used to some extent as an initiator codon, only a dipeptide could have been formed due to the neighborhood of a terminator UGA. As is generally accepted (5, 8, 15), initiation at an upstream AUG should interfere with the expression of the polyprotein ORF. Accordingly, the closer to the optimal is the context of the upstream AUG within the insert, the less efficient is the viral reproduction that could be expected. The very high level of attenuation of mutant 83 (aauAUGu), which has a purine (A) at the −3 position, complied with this expectation, since this position is considered to have a dominant effect among other positions of the AUG context and the A_{-3} residue endows the context with the highest strength (13).

The properties of other mutants, however, appeared to contradict this rule. Mutants with a −3 pyrimidine but having a purine (G) residue in the +4 position of the upstream AUG elicited a more severe clinical pattern than the mutants with a less favorable pyrimidine (C or U) residue. This fact suggests that upstream AUGs with a stronger context may, contrary to expectations, exert less interference with the polyprotein translation. Although the mechanism ensuring such an apparently paradoxical sensitivity of the translation initiation machinery of relevant CNS cells to the nucleotide in the +4 position of an upstream AUG is unknown, two hypothetical explanations may be put forward. Either the noninitiating AUGs with a G_{+4}-containing context within the starting window facilitate formation of a productive ribosome-template complex (23), or such a context promotes synthesis of the dipeptide followed by reinitiation at the cognate initiator AUG, as is known to occur in some cases after translation of an upstream ORF (12, 14, 19).

Whatever the molecular mechanism, the finding of distinct attenuation phenotypes caused by changing the context of an upstream AUG within the translational starting window was an important and unexpected observation. Especially intriguing were the apparently separate effects of appropriate mutations on the morbidity (as judged by PD_{50}s) and mortality rates caused by the mutant-induced infections. We are not aware of a similar phenotypic effect of any other mutations in any other neurovirulent viruses. Although the difference between the clinical phenotypes of the mutants could partly be attributed to a likely slower growth and/or spread of the mutants with a +4 pyrimidine (mutants 43 and 64) compared to G_{+4}-containing mutants (mutants 63 and 65), several lines of indirect evidence suggested that some qualitative rather than merely quantitative distinctions in the virus-host interaction were also involved. Thus, the probability of apparent recovery of mutant 43- and 64-inoculated mice did not decrease with a shorter incubation period, suggesting that a relatively benign progression of the infection was an inherent property of these viruses. The enhanced immune response could hardly fully explain the relative mildness and reversibility of neurologic symptoms induced by the viruses, since the rare emergence of more virulent revertants resulted in severe, irrecoverable paralytic disease. The significant inflammatory reaction in the white matter of mutant 43- and 64-infected mice in the absence of detectable viral antigen (an intriguing and enigmatic finding) could well contribute to the clinical manifestations and might, for example, be responsible for the disproportionately low PD_{50}s and the second wave of paralytic symptoms observed in some cases.

Another important aspect of this study concerned the absence of persistence, which is characteristic of BeAn or DA strains, in mice infected with attenuated, nonlethal mutants of the GDVII strain of TMEV, a notion discussed in more detail elsewhere (11, 18). This finding is in line with previous results demonstrating that the relevant capacities of BeAn and DA strains of this virus are due largely, if not exclusively, to point mutations in the viral capsid (1, 10, 16). Thus, the same virus can induce quite different diseases depending on minute changes in coding (GDVII versus BeAn and DA strains) and noncoding (GDVII and mutants 63 and 65 versus mutants 43 and 64) parts of its genome. Such a variability in the mortality, morbidity, and clinical patterns elicited by virus variants differing from one another by only a few point mutations spread over the viral genome is certainly not a unique property of TMEV. It can likely be extrapolated to different viruses that are pathogenic for humans and should be taken into consideration in studies on viral pathogenesis as well as in laboratory identification of viruses.

ACKNOWLEDGMENTS

This study has been supported in part by grants form the Russian Foundation for Basic Research (96-04-48131, 96-15-97024, and 96-15-97867), CRDF (RB1-271), Institut Pasteur Foundation, the Centre National de la Recherche Scientifique, and the EC Human Capital and Mobility Program (contract no. CHRX-CT94-0670). Short-term visits of E.G.V. to the Pasteur Institut were supported by the French Embassy in Moscow.

REFERENCES

1. **Adami, C., A. E. Pritchard, T. Knauf, M. Luo, and H. L. Lipton.** 1998. A determinant for central nervous system persistence localized in the capsid of Theiler's murine encephalomyelitis virus by using recombinant viruses. J. Virol. **72:**1662–1665.
2. **Agol, V. I.** 1991. The 5′-untranslated region of picornaviral genomes. Adv. Virus Res. **40:**103–180.
3. **Agol, V. I., E. V. Pilipenko, and O. R. Slobodskaya.** 1996. Modification of translation control elements as a new approach to design of attenuated picornavirus strains. J. Biotechnol. **44:**119–128.
4. **Aubert, C., M. Chamorro, and M. Brahic.** 1987. Identification of Theiler's virus infected cells in the central nervous system of the mouse during demyelinating disease. Microb. Pathog. **3:**319–326.
5. **Cao, J., and A. P. Geballe.** 1995. Translation inhibition by a human cytomegalovirus upstream open reading frame despite inefficient utilization of its AUG codon. J. Virol. **69:**1030–1036.
6. **Chomczynski, P., and N. Sacchi.** 1987. Single-step method of RNA isolation by acid guanidinium thiocyanate-phenol-chloroform extraction. Anal. Biochem. **162:**156–159.
7. **Dal Canto, M. C., R. W. Melvold, B. S. Kim, and S. D. Miller.** 1995. Two models of multiple sclerosis: experimental allergic encephalomyelitis (EAE) and Theiler's murine encephalomyelitis virus (TMEV) infection—a pathological and immunological comparison. J. Microsc. Res. Tech. **32:**215–229.
8. **Geballe, A. P., and D. R. Morris.** 1994. Initiation codons within 5′-leader of mRNAs as regulators of translation. Trends Biochem Sci. **19:**159–164.
9. **Jackson, R. J., and A. Kaminski.** 1995. Internal initiation of translation in eukaryotes: the picornavirus paradigm and beyond. RNA **1:**985–1000.
10. **Jarousse, N., C. Martinat, S. Syan, M. Brahic, and A. McAlister.** 1996. Role of VP2 amino acid 141 in tropism of Theiler's virus within the central nervous system. J. Virol. **70:**8213–8217.
11. **Jarousse, N., E. G. Viktorova, E. V. Pilipenko, V. I. Agol, and M. Brahic.** 1999. An attenuated variant of the GDVII strain of Theiler's virus does not persist and does not infect the white matter of the central nervous system. J. Virol. **73:**801–804.
12. **Kozak, M.** 1984. Selection of initiation sites by eucaryotic ribosomes: effect of inserting AUG triplets upstream from the coding sequence for preproin-

sulin. Nucleic Acids Res. **12:**3873–3893.
13. **Kozak, M.** 1986. Point mutations define a sequence flanking the AUG initiator codon that modulates translation by eukaryotic ribosomes. Cell **44:**283–292.
14. **Kozak, M.** 1987. Effects of intercistronic length on the efficiency of reinitiation by eucaryotic ribosomes. Mol. Cell. Biol. **7:**3438–3445.
15. **Kozak, M.** 1989. The scanning model for translation: an update. J. Cell Biol. **108:**229–241.
16. **Lin, X., S. Sato, A. K. Patick, L. R. Pease, R. P. Roos, and M. Rodriguez.** 1998. Molecular characterization of a nondemyelinating variant of Daniel's strain of Theiler's virus isolated from a persistently infected glioma cell line. J. Virol. **72:**1262–1269.
17. **Lipton, H. L., and M. L. Jelachich.** 1997. Molecular pathogenesis of Theiler's murine encephalomyelitis virus-induced demyelinating disease in mice. Intervirology **40:**143–152.
18. **Lipton, H. L., A. E. Pritchard, and M. A. Calenoff.** 1998. Attenuation of neurovirulence of Theiler's murine encephalomyelitis virus strain GDVII is not sufficient to establish persistence in the central nervous system. J. Gen. Virol. **79:**1001–1004.
19. **Luukkonen, B. G. M., W. Tan, and S. Schwartz.** 1995. Efficiency of reinitiation of translation on human immunodeficiency virus type 1 mRNAs is determined by the length of the upstream open reading frame and by intercistronic distance. J. Virol. **69:**4086–4094.
20. **Miller, D. J., and M. Rodriguez.** 1995. Spontaneous and induced remyelination in multiple sclerosis and the Theiler's virus model of central nervous system demyelination. Microsc. Res. Tech. **32:**230–245.
21. **Pilipenko, E. V., V. M. Blinov, B. K. Chernov, T. M. Dmitrieva, and V. I. Agol.** 1989. Conservation of the secondary structure elements of the 5′-untranslated region of cardio- and aphthovirus RNAs. Nucleic Acids Res. **17:**5701–5711.
22. **Pilipenko, E. V., A. P. Gmyl, S. V. Maslova, Y. V. Svitkin, A. N. Sinyakov, and V. I. Agol.** 1992. Procaryotic-like *cis* element in the cap-independent internal initiation of translation on picornavirus RNA. Cell **68:**119–131.
23. **Pilipenko, E. V., A. P. Gmyl, S. V. Maslova, G. A. Belov, A. N. Sinyakov, M. T. Huang, D. K. Brown, and V. I. Agol.** 1994. Starting window, a distinct element in the cap-independent internal initiation of translation on picornaviral RNA. J. Mol. Biol. **241:**398–414.
24. **Pilipenko, E. V., A. P. Gmyl, S. V. Maslova, E. V. Khitrina, and V. I. Agol.** 1995. Attenuation of Theiler's murine encephalomyelitis virus by modifications of the oligopyrimidine/AUG tandem, a host-dependent translational *cis* element. J. Virol. **69:**864–870.
25. **Rueckert, R. R.** 1995. Picornaviridae: the viruses and their replication, p. 477–522. *In* B. N. Field, D. M. Knipe, and P. M. Howley (ed.), Fundamental virology. Lippincott-Raven, Philadelphia, Pa.
26. **Svitkin, Y. V., S. V. Maslova, and V. I. Agol.** 1985. The genomes of attenuated and virulent poliovirus strains differ in their *in vitro* translation efficiencies. Virology **147:**243–252.
27. **Svitkin, Y. V., T. V. Pestova, S. V. Maslova, and V. I. Agol.** 1988. Point mutations modify the response of poliovirus RNA to a translation initiation factor: a comparison of neurovirulent and attenuated strains. Virology **166:** 394–404.
28. **Tsunoda, I., and R. S. Fujinami.** 1996. Two models for multiple sclerosis: experimental allergic encephalomyelitis and Theiler's murine encephalomyelitis virus. Neuropathol. Exp. Neurol. **55:**673–686.
29. **Wimmer, E., C. U. T. Hellen, and X. Cao.** 1993. Genetics of poliovirus. Annu. Rev. Genet. **27:**353–436.